ELSEVIER

Chemical Engineering Journal 86 (2002) 11–15

Chemical Engineering Journal

www.elsevier.com/locate/cej

New simple mathematical model of a honeycomb rotary absorption-type dehumidifier

Wiwut Tanthapanichakoon*, Anawut Prawarnpit

Faculty of Engineering, Department of Chemical Engineering, Chulalongkorn University, Patumwan, Bangkok 10330, Thailand

Abstract

A simplified mathematical model consisting of ordinary differential equations has been proposed and found to accurately predict the dynamic performance of a honeycomb rotary absorption-type dehumidifier in a beverage factory. The model was validated experimentally using the transient measurement data on the air properties at the outlets of both the dehumidification and regeneration sections. Good agreement between the predicted and recorded data at each time has been observed. The model is numerically stable and easy to simulate.

Keywords: Rotary dehumidifier; Honeycomb; Lithium chloride salt; Solid absorbent; Dynamic model

1. Introduction

For hygienic reasons the equipment as well as the floor space in the concentrate preparation room of a modern beverage factory are daily cleaned, scrubbed, mopped and left to dry-out overnight. To dehumidify the circulating humid air and ensure the dry-out of the wet floor in the closed room, the present factory employs two identical continuous rotary dehumidifiers. In contrast to adsorption-type dehumidifiers that use silica gel, molecular sieve, etc. as adsorbent, the tested absorption-type dehumidifier uses a lithium chloride-coated honeycomb. As the rotor slowly turns, humid room air is circulated through and dehumidified in the absorption section of the honeycomb. Meantime ambient air is heated to about 350 K and simultaneously sent counter-current through the regeneration section to dry the moist solid absorbent.

In the past all investigations have focussed on the adsorption-type rotary dehumidifier and there are no publications on the rotary absorption type. Kodama et al. [1–3] experimentally investigated the temperature effect and optimal operation of a thermal-swing honeycomb rotor adsorber. To predict simultaneous heat and mass performance of the regenerator of a rotary dehumidifier, Maclaine-cross and Banks [4] and Banks [5,6] utilized linear and nonlinear analogy method, whereas Mathiprakasam and Lavan [7] predicted the performance of adiabatic desiccant dehumidifiers using linear solutions. These earlier methods are handy but not so rigorous and did not provide detailed or transient information.

To numerically solve the governing partial differential equations of a rotary adsorption-type dehumidifier, Holmberg [8], Jurinak and Mitchell [9] and Schultz and Mitchell [10] developed and applied an explicit-finite difference technique. To ensure unconditional numerical stability and reduce computational time, Zheng and Worek [11] proposed and applied an implicit-finite difference technique for the numerical simulation.

In contrast the authors have developed a new, simple dynamic model for the honeycomb rotary dehumidifier consisting of a set of nonlinear ordinary differential equations. The validity of the present model was substantiated by comparing the simulated results with the transient experimental values. The model accuracy with respect to the key variables (outlet and inlet air temperatures and humidities) is better than ±2%.

2. Mathematical model of rotary dehumidifier

A typical honeycomb rotor consists of thousands of almost identical narrow straight slots uniformly distributed over its rotor cross-section as shown in Fig. 1. Because of geometric similarity, the multiple annular layers of straight slots in the dehumidification and the regeneration sections can be represented by a "representative annulus" of thickness Δr equaling one slot height. In this way, the three cylindrical coordinates (r, θ, z), say radial, angular and axial directions,

* Corresponding author. Fax: +66-2-218-6894.
E-mail address: twiwut@chula.ac.th (W. Tanthapanichakoon).

1385-8947/02/$ – see front matter
PII: S1385-8947(01)00266-2

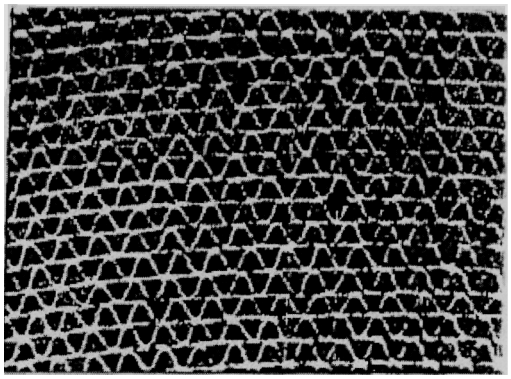

Fig. 1. Honeycomb structure.

respectively, in the model can rationally be reduced to the two coordinates (θ, z). By taking into account each constituent slot within the total M identical slots in the θ-direction spanning the entire cross-section of the representative annulus, the remaining space variable is z. For example, $M = 400$ with the first 100 slots being the regeneration section. Of course, a second independent variable in the model is the time t. In other words, the dynamic behavior of the honeycomb rotor can be simulated by following the transient changes occurring in the z-direction within each of the M slots as the rotor slowly turns.

The following simplifying assumptions are made:

1. Air flow is uniformly distributed across the dehumidification and the regeneration cross-sections.
2. The air stream flowing through each slot is assumed to be plug or piston flow. In the plug flow model, variation does not exist in the radial direction but exists only in the axial or z-direction. Theoretically and conceptually, the plug flow model has been shown to be equivalent to the model of a series of equal-volume CSTRs in which an infinitely large number of completely mixed cells, each of infinitely small thickness, are connected in series. For practical reasons, the plug flow model of each slot will be approximated by an equivalent CSTR model consisting of N cells in series as shown in Fig. 2, N being 10, 20 or more [12].
3. Gas-phase heat conduction and mass diffusion in the axial direction are negligibly small compared to the convective effects in the same slot.
4. Each slot is adiabatic and heat conduction along the slot wall may be neglected.
5. Interphase moisture transfer between the gas and solid absorbent phases in the slot is controlled by gas-phase film resistance since the absorbent layer is essentially non-porous.
6. Heat of absorption of the moisture can be approximated by the latent heat of vaporization of water.

For slot no. j of the regeneration section ($j = 1, 2, \ldots, M_r$), the unsteady mass and energy balances for cell no. i ($i = 1, 2, \ldots, N$) are as follows:

Gas-phase moisture balance:

$$\frac{d(H_i)}{dt} = \frac{NG_{Fa}V_{Hi}}{L}(H_{i-1} - H_i) - \frac{kA_hNV_{Hi}}{\varepsilon LA_c}(H_i - H_{Si}) + \left(\frac{H_i}{V_{Hi}}\right)\frac{d(V_{Hi})}{dt} \quad (1)$$

where H_i and H_{Si} are the humidity and saturated humidity of hot air in cell no. i, respectively ($kg_{water\ vapor}\ kg_{dry\ air}^{-1}$), V_{Hi} the specific volume of humid air ($m^3\ kg_{dry\ air}^{-1}$), G_{Fa} the mass flow rate of humid air ($kg_{dry\ air}\ m^{-2}\ s^{-1}$), t the time (s), L the length of each rotor slot, N represents the number of cells in each slot, k the mass transfer coefficient between moist material and hot air ($kg\ m^{-2}\ s^{-1}$), ε the honeycomb porosity (–), A_h the internal surface area of each cell (m^2), A_c the total cross-sectional area of each cell (m^2). The Ranz–Marshall correlation is used to estimate the value of k [13].

Solid-phase moisture balance:

$$\frac{d(W_i)}{dt} = k(H_i - H_{Si})\frac{NA_h}{LA_c\rho_{SB}} \quad (2)$$

where W_i is the moisture in the absorbent material in cell i ($kg_{water}\ kg_{dry\ material}^{-1}$), ρ_{SB} the apparent density of dry absorbent material in the rotor ($kg\ m^{-3}$).

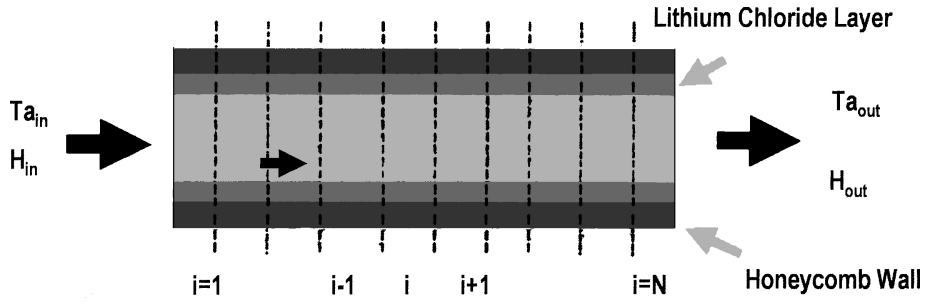

Fig. 2. Representation of a typical honeycomb slot as a series of completely mixed cells.

Gas-phase energy balance:

$$\left(\frac{C_{pA}+C_{pv}H_i}{V_{Hi}}\right)\frac{d(T_{Ai})}{dt} = \frac{NG_{Fa}}{L}(C_{pA}+C_{pv}H_{i-1})(T_{A(i-1)}-T_{Ai}) - \frac{h_c N A_h}{\varepsilon A_c L}(T_{Ai}-T_{Si}) + \left(\frac{kA_hN}{\varepsilon LA_c}\right)(H_i-H_{Si}) \times (C_{pw}T_{Si}+C_{pv}(T_{Ai}-T_{Si})) + \left(\frac{C_{pA}T_{Ai}}{V_{Hi}^2}\right)\frac{d(V_{Hi})}{dt} \quad (3)$$

where C_{pA}, C_{pv}, C_{pw} are the specific heat of dry air, water vapor and liquid water, respectively (kJ kg^{-1} K^{-1}), T_{Ai} and T_{Si} are the temperatures of humid air and solid absorbent in cell no. i, respectively (K), h_c the heat transfer coefficient between the gas- and solid-phase (kJ m^{-2} s^{-1}).

Solid-phase energy balance:

$$(\rho_{FB}C_{pFB}+\rho_{SB}C_{pSB}+\rho_{SB}C_{pw}W_i)\frac{d(T_{Si})}{dt} = \left(\frac{kA_hN}{LA_c}\right)(H_i-H_{Si})(\lambda_{Si}-C_{pw}T_{Si}) + \frac{h_cA_hN}{LA_c}(T_{Ai}-T_{Si}) \quad (4)$$

where λ_{Si} is the latent heat of vaporization at temperature T_{Si} in cell no. i (kJ kg$_{water}^{-1}$), ρ_{FB} the apparent density of honeycomb wall (kg m^{-3}).

It should be noted that a similar set of equations is applicable to the slots in the dehumidification section ($j = 101, 102, \ldots, 400$), except that the air flow direction is reversed.

Air circulation during the night inside the closed room can be approximated as a series of R imaginary completely mixed compartments ($R = 2$–4). Here R is the number of compartments in the room. As dehumidified air circulates through the room, it picks up moisture from the wet concrete floor thus gradually drying out the floor. Because of space limitation the model equations for the room are omitted here. The fourth order Runge–Kutta method is used to integrate the set of four ($MN + R$) ordinary differential equations simultaneously. By choosing the time step of integration appropriately, at the end of each time step, slot no. j will rotate to replace the next slot $j + 1$ successively in circle. Similarly, slot no. M will replace slot no. 1 after each time step.

3. Experimental

The tested honeycomb rotor [14] has a 52.5 cm diameter and 10 cm width. Fig. 3 shows a schematic diagram of the honeycomb rotor dehumidifier. The area ratio of the dehumidification to the regeneration section is 3:1. The rotary dehumidifier is operated overnight in a closed room with 45 m^2 floor area. Temperature of the heat ambient air entering the regeneration section is set constant at 350 K. Wet- and dry-bulb temperatures of the ambient air (before the air heater) of room and dehumidified air at the outlet of the absorption section were recorded continuously. The air

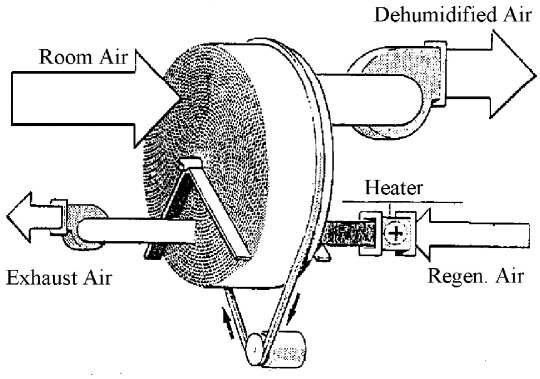

Fig. 3. Schematic diagram of honeycomb rotor dehumidifier.

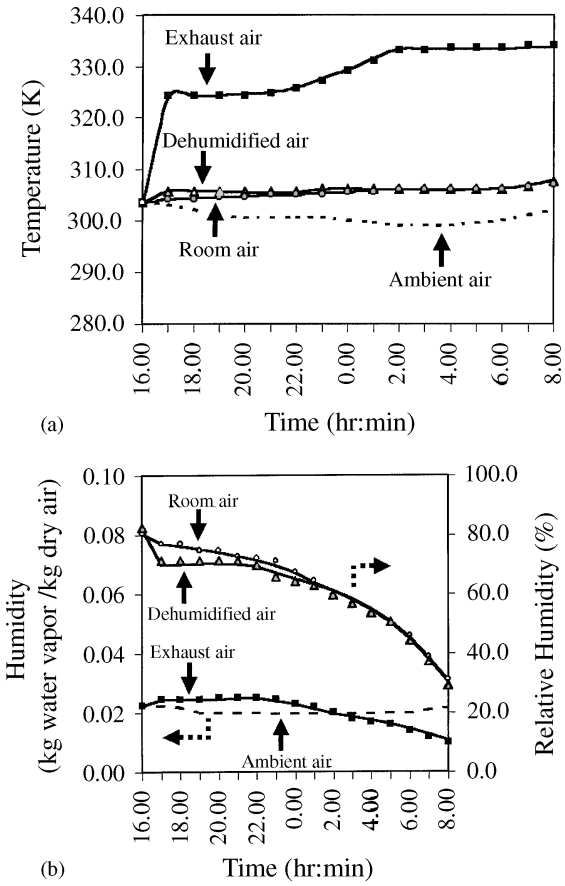

Fig. 4. (a) Comparison of the predicted air temperatures with the experimental results (T_{regen} = 353 K, $v_{abs,in}$ = 1.37 m/s, $v_{regen,in}$ = 1.01 m/s, rotational speed = 10 rph); (b) comparison of the predicted air and relative humidities with the experimental results (T_{regen} = 353 K, $v_{abs,in}$ = 1.37 m/s, $v_{regen,in}$ = 1.01 m/s, rotational speed = 10 rph).

flow rates across the absorption and regeneration sections are 22 and 5.4 m^3/s, respectively.

4. Results and discussion

The observed ambient air conditions are used as time-dependent inputs to the heater of the regeneration section. Since the room is completely closed off at night, only the initial conditions in the room at the start of operation of the rotary dehumidifier are needed to run the simulation. Fig. 4 shows a typical example of the ambient air (broken line) and the simulated (solid line) vs. experimental values (dots) of the various air temperatures and humidities. Evidently the predicted and observed values of the dehumidified (absorption outlet), room and exhaust air (regeneration outlet) are in very good agreement. Though not shown here, additional tests carried out on several other days

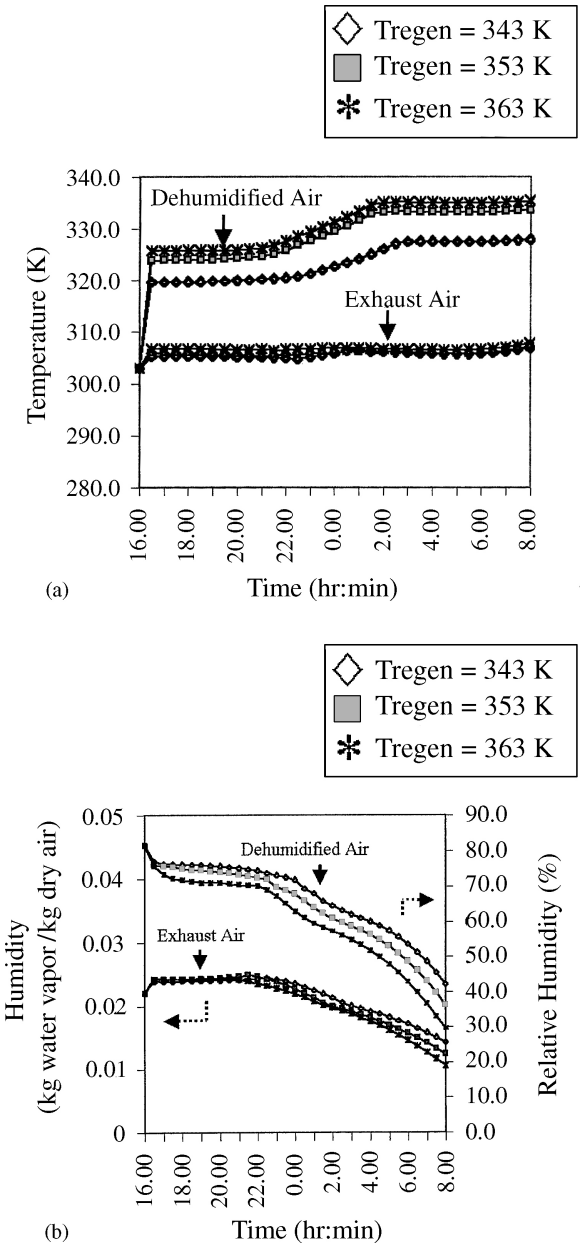

Fig. 5. (a) Comparison of the predicted air temperatures at various regenerated temperatures ($v_{abs,in}$ = 1.37 m/s, $v_{regen,in}$ = 1.01 m/s, rotational speed = 10 rph); (b) comparison of the predicted air and relative humidities at various regenerated temperatures ($v_{abs,in}$ = 1.37 m/s, $v_{regen,in}$ = 1.01 m/s, rotational speed = 10 rph).

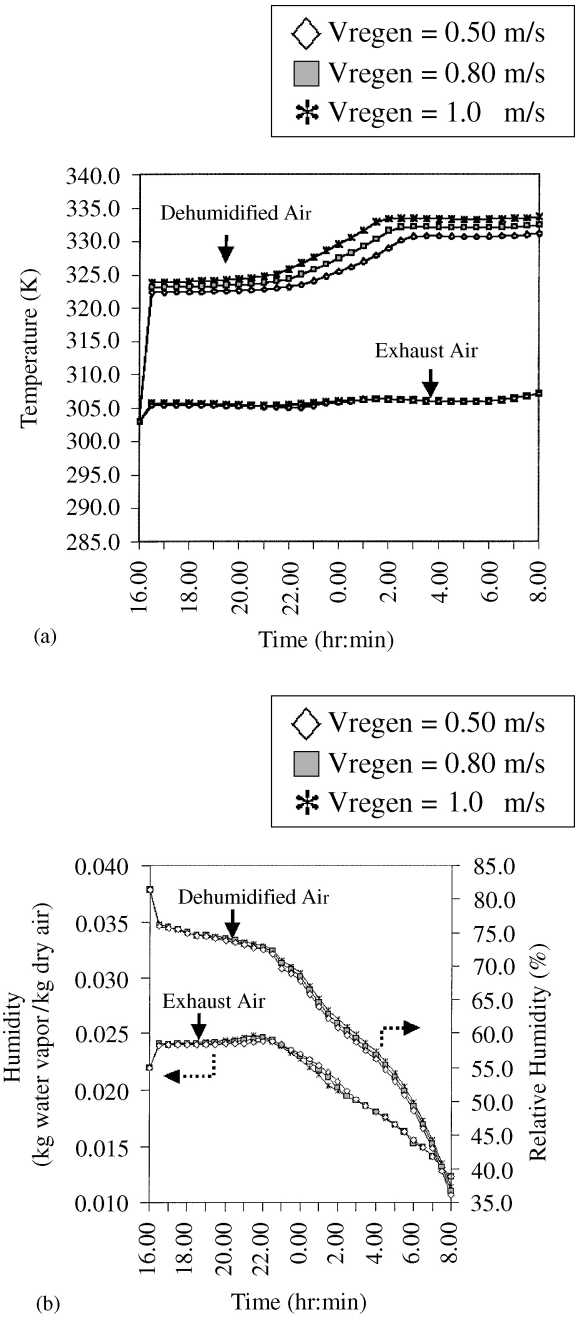

Fig. 6. (a) Comparison of the predicted air temperatures at various regenerated velocities (T_{regen} = 353 K, $v_{abs,in}$ = 1.37 m/s, rotational speed = 10 rph); (b) comparison of the predicted air and relative humidities at various regenerated velocities (T_{regen} = 353 K, $v_{abs,in}$ = 1.37 m/s, rotational speed = 10 rph).

also gave the same good agreement. Thus it may be concluded that a simple dynamic model for the honeycomb rotary dehumidifier has successfully been developed and validated.

Next the effects of the regenerator's inlet air temperature and velocity on the efficiency of dehumidification are investigated. As shown in Fig. 5, the temperature and humidity of both the dehumidified and exhaust air depend significantly on the regenerator's inlet air temperature. Obviously, the humidity of room air can be reduced faster at a higher regenerator's temperature. The effect of the regenerator's air velocity is shown in Fig. 6. It can be seen that the air velocity has insignificant influence on the dehumidification efficiency.

5. Conclusion

The new simple dynamic model has been shown to simulate the dynamic performance of a honeycomb rotary dehumidifier that agrees well with experimental results. Though the model was developed and validated for an absorption-type dehumidifier, the approach should also be applicable to the adsorption-type dehumidifier. Coupled with a simple model for the humid air in a closed room with wet floor, the present model has also proved successful in predicting the property change in the room air and the decreasing amount of water remaining on the wet concrete floor. In the next investigation, the coupled models will be used to obtain an optimal set of operating conditions that minimizes the energy and/or time required to dry-out the wet floor overnight.

Acknowledgements

Financial support from Thailand Research Fund (Senior Research Scholar Program) for WT is gratefully acknowledged. Preparation of the manuscript is aided by Ornjira Rungarunsangchai who also received partial financial support from the same TRF Program.

References

[1] A. Kodama, M. Goto, T. Hirose, T. Kuma, J. Chem. Eng. Jpn. 26 (1993) 530–535.
[2] A. Kodama, M. Goto, T. Hirose, T. Kuma, J. Chem. Eng. Jpn. 27 (1994) 644–649.
[3] A. Kodama, M. Goto, T. Hirose, T. Kuma, J. Chem. Eng. Jpn. 28 (1995) 19–24.
[4] I.L. Maclaine-cross, P.J. Banks, Int. J. Heat Mass Transfer 15 (6) (1972) 1225–1242.
[5] P.J. Banks, ASME J. Heat Transfer 107 (1985) 222–229.
[6] P.J. Banks, ASME J. Heat Transfer 107 (1985) 230–238.
[7] B. Mathiprakasam, Z. Lavan, ASME J. Solar Energy Eng. 102 (1980) 73–79.
[8] R.B. Holmberg, ASME J. Heat Transfer 101 (1979) 205–210.
[9] J.J. Jurinak, J.W. Mitchell, J. Heat Transfer Trans. ASME 106 (1984) 638–645.
[10] K.J. Schultz, J.W. Mitchell, ASME J. Solar Energy Eng. 111 (1989) 286–291.
[11] W. Zheng, W.M. Worek, Numer. Heat Transfer A 23 (1993) 211–232.
[12] D.M. Himmelbleu, K.B. Bischoff, Process Analysis and Simulation, Wiley, New York, 1970.
[13] J.H. Perry, Chemical Engineers' Handbook, 3rd Edition, McGraw-Hill, New York, 1958.
[14] A. Prawarnpit, Simulation of rotary adsorption dehumidifier system, M.S. Thesis, Department of Chemical Engineering, Chulalongkorn University, Bangkok, Thailand, 1999.